COMPUTER-OPTIMIZED DESIGN OF QUARTER-WAVE ACOUSTIC MATCHING AND ELECTRICAL MATCHING NETWORKS FOR ACOUSTIC TRANSDUCERS

A. R. Selfridge, R. Baer, B. T. Khuri-Yakub, and G. S. Kino

Ginzton Laboratory
Stanford University
Stanford, California 94305

Abstract

We have developed an iterative computer program to optimize the parameters for the acoustic matching layer(s) and the electrical matching network of a transducer for a minimum length of the impulse response. By including the interactions between electrical and acoustic matching in our model, we have been able to significantly improve the quality of our transducers.

A 3.65 MHz center frequency transducer, made of Murata PZT, was constructed to verify the computer results. The impulse response was approximately 2-1/2 cycles long with a round trip insertion loss of 10.9 dB at the center frequency, and the 40 dB ringdown time was 1.5 μsec when working into a water load.

Introduction

Electrical matching networks are often used between acoustic transducers and their electrical sources to improve efficiency and tailor the bandshape of the overall system. Matching networks have been made for SAW devices which provide a flat bandshape for example. This paper describes the design of transducers with a short impulse response as well as low insertion loss. We show that the iterative techniques used in the past[1-4] to design electrical matching circuits for acoustic transducers can also be used to obtain the optimal acoustic parameters for an acoustic matching layer at the same time. This technique has proven to be very effective in improving the overall response of the transducer and tuning network system.

An accurate transducer model must be used to calculate the effect of changes in the acoustic parameters, which in our case are the thickness and impedance of a matching layer. For this purpose we have used the KLM[5,6] model.

An initial set of design parameters, algorithms for varying them, and algorithms by which to rate a given set of design parameters are also needed. We will describe the algorithms we use, and show the results we have obtained.

The Problem

Consider the transducer system shown schematically in Fig. 1. The system can be broken down into three basic parts: the electromechanical transducer, the matching network, and the driving (and receiving) source. The problem we are faced with is how to choose the best values for all of the variables listed over the respective boxes shown in Fig. 1. In this example the transducer area, backing impedance, piezoelectric material, and frequency are considered as fixed by the application. For simplicity, there is only one matching layer. The techniques to be described, however, have also been employed to design two matching layer devices with good results.

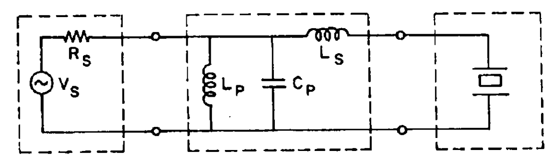

Fig. 1. Transducer and driving network to be optimized.

Proper choice of the listed design parameters requires a clear understanding of the most desirable properties of the transducer and matching network. We regard optimum performance to be obtained by minimizing both the long term ringing after the impulse response as well as the insertion loss.

These properties are easy to evaluate in the time domain, though somewhat elusive in the frequency domain. For this reason the criterion we have chosen to use is based on the calculated impulse response of the system $h(t)$. We define a "badness" criterion as follows

$$b = \text{"badness"} = \frac{\int_{t_0}^{\infty} |h(t)|(t - t_0)dt}{S^2} \qquad (1)$$

where "S" is the peak amplitude of the impulse response and t_0 is, as Fig. 2 indicates, the time of the fifth zero crossing in the impulse response.

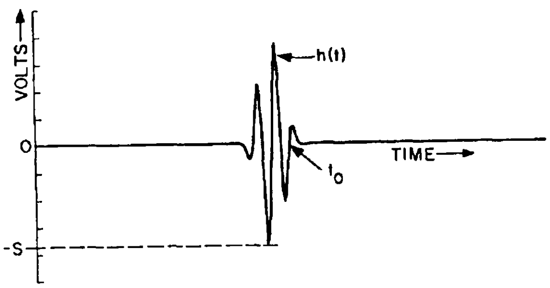

Fig. 2. Example of impulse response from which "badness" is calculated.

By adjusting the various design parameters, our iterative routine tries to minimize the "badness" as calculated using Eq. (1). This is accomplished either by reducing the time weighted ringing after t_0, or increasing the peak amplitude of the impulse response, or hopefully both. The factor of S^2 in the denominator of Eq. (1) reflects the fact that we need one power of S to normalize the integral of the ringing, and another power of S to emphasize the reduction of the overall insertion loss. Higher powers of S were tried with predictable results. Use of S^3 would result in a larger peak amplitude impulse responses with more ringing for example.

The choice of t_0 in Eq. (1) deserves some explanation. At first t_0 was chosen to be at the very beginning of the impulse response. When this value of t_0 is used, the result of iterating is to increase the center frequency of the transducer, matching network system. This had the effect of reducing the width of the impulse response, though not the overall number of cycles. This was deemed an inappropriate use of the degrees of freedom in the transducer design, and hence only the energy after the first 2-1/2 cycles is treated as undesirable.

Another problem with computer adaption of this type was observed when t_0 was set equal to the time of the sixth zero crossing. In this run, the computer converged upon a design with an ugly impulse response, which was distorted in such a way as to delay the sixth zero crossing as much as possible. Problems such as this are indicated by rapid changes in "badness" due to relatively minor changes in a design parameter. Obviously it is necessary to be aware of all these subtleties and be prepared to change t_0 under different circumstances. For example, if we were optimizing a heavily damped transducer with typically a 3/2 cycle response, we might have to choose t_0 to be the time of the second zero crossing.

Initial Choice and Variation of Design Parameters

The "badness" function has 6 input variables and a single, real and positive output value. It can be visualized as a surface over 6 space. We would like to find the global minimum in this surface, or the set of 6 design parameters which yield a transducer design with the minimum badness. Unfortunately, the badness function takes about 5 seconds of computer time to evaluate, and it could take many years to evaluate the badness function over a grid fine enough to ensure that the global minimum would be found. To overcome this problem, computer optimization techniques are used to find minima in the badness surface. They require the choice of initial values of the design parameters, and algorithms with which to vary them. They do not insure, however, that any of the minima they find is the global minimum. For the case of longitudinal wave transducer working into water, the best results so far have been achieved by simply starting the optimizations from the points in 6 space which correspond to our previous and simpler design theory.

Thus, we used the values derived by DeSilets et al,[5] which calls for a matching layer a quarter wavelength long at the center frequency with an impedance

$$Z_\ell = (Z_c Z_w^2)^{1/3} \tag{2}$$

where Z_c is the stiffened impedance of the ceramic, and Z_w is the longitudinal plane wave impedance of water, or $1.5 \times 10^6\ \mathrm{kg/m^2 s}$.

The initial values chosen for the matching elements, shown in Fig. 1, were

$$C_p = C_0; \quad L_p = L_s = \frac{1}{\omega_0^2 C_0} \tag{3}$$

These values do not yield a very good initial design, though the optimization procedures work well from here.

We next describe the algorithms required to follow the gradients in 6 space to the nearest minimum. The optimization routines in use at present adjust only one parameter at a time. Other techniques, such as the method of steepest descent could have been used. However, the simple approach described here seems to work quite well, and avoids certain difficulties that occur with the method of steepest descent when the gradients are small.

We treat the badness parameter, b, as a function of one of the design parameters β_n. We assume, for the time, that b can be adequately approximated by the first three terms of its Taylor series expansion, i.e.,

$$b(\beta_n + \Delta\beta_n) = b(\beta_n) + \Delta\beta_n \frac{\partial b}{\partial \beta_n} + \frac{\Delta\beta_n^2}{2!} \frac{\partial^2 b}{\partial \beta_n^2} \tag{4}$$

Thus we can express the change in badness due to a change in the nth design parameter as

$$\Delta b = \Delta\beta_n \frac{\partial b}{\partial\beta_n} + \frac{(\Delta\beta_n)^2}{2} \frac{\partial^2 b}{\partial\beta_n^2} \tag{5}$$

We wish to choose $\Delta\beta_n$ so as to reduce b. This implies that we must make changes in β_n such that $\Delta b < 0$. If we make

$$\Delta\beta_n = -\alpha_n \frac{\partial b}{\partial\beta_n} \tag{6}$$

where $\alpha_n > 0$, then the first order change in b will always be negative. However, the second order change may be in either direction. The choice of Eq. (6), when substituted into Eq. (5), gives the result

$$\Delta b = -\alpha_n \left(\frac{\partial b}{\partial\beta_n}\right)^2 \left(1 - \frac{\alpha_n}{2} \frac{\partial^2 b}{\partial\beta_n^2}\right) \tag{7}$$

If the change in $\Delta\beta_n$ is going to decrease the badness b, then we must have $\Delta b < 0$. From Eq. 7 we can see that this indeed will be the case, even if $\partial^2 b/\partial\beta_n^2$ is positive, provided

$$\alpha_n < \frac{2}{\dfrac{\partial^2 b}{\partial\beta_n^2}} \tag{8}$$

The second derivative will, in fact, be positive when b is approaching a minimum value rather than a maximum. If we differentiate Eq. (7) with respect to α_n, and set the derivative to zero, we obtain the value of α_n for the maximum change of badness to be

$$\alpha_n = \frac{1}{\dfrac{\partial^2 b}{\partial\beta_n^2}} \tag{9}$$

With Eq. (6) and Eq. (9), we can calculate the appropriate change to the nth design parameter. After calculating $\Delta\beta_n$, it is tested to see if it is too big and reduced to a reasonable size if it is. Next, the resulting value of β_n is tested to see if it yields a reduced badness parameter. If it does, this new value is retained and the computation goes on to the next parameter. If b is not smaller, the best point obtained in the computation is retained and the corresponding value of β_n is used. Next n is incremented and the procedure is repeated for the $n + 1$ design parameter. After all n parameters have been adjusted, the computation begins again with β_1 unless a specified number of iterations have been completed.

Experimental Results

We have designed and constructed a 3.65 MHz bulk wave transducer on a low-impedance lossy epoxy backing ($Z_B = 3.3 \times 10^6$ kg/m²sec), working into a water load with impedance 1.5×10^6 kg/m²sec. A single acoustic matching layer was used on the front acoustic port, and a three-component electrical matching network, like the one shown in Fig. 1, was used on the electrical port. The active element in the transducer was 0.470 inch diameter disk of Murata PZT. This disk was 0.0255 inches thick, and electroded on both of its circular surfaces.

The first step in designing this bulk wave transducer was to accurately measure the appropriate piezoelectric parameters of this new Murata material. We obtained the following parameters: stiffened, longitudinal wave velocity, after repoling, $v^D = 4.72$ mm/μs; density, $\rho = 7.95 \times 10^3$ kg/m³; dielectric constant, $\epsilon_{33}^S = 200\ \epsilon_0$; electromechanical coupling coefficient, $k_T^2 = 0.24$; lumped mechanical and electrical $Q \approx 4000$.

Using these material properties for the active element, the iterative techniques of the previous section determined that an optimal matching layer would have an impedance of 3.45×10^6 kg/m²sec, and thickness of 0.243 wavelengths at the center frequency. The optimized values for the electrical components in the transducer system were

$$L_s = 5.38\ \mu H \qquad L_p = 7.37\ \mu H$$
$$C_p = 360\ pF \qquad R_s = 85.2\ \Omega \tag{10}$$

The first step used in fabricating the transducer was to bond the active element to the backing. The electrical impedance of the active element on a backing was made at this point to verify the previously measured values of v^D and k_T^2. These parameters had been difficult to measure in this high Q material owing, we believe, to a thickness variation in the PZT disk of about 1%. By backing the disk, many of the spurious modes are damped out. While it is impossible to measure Q in this case, measurement of v^D, ϵ_{33}^S, and k_T^2 can be much simpler. Excellent agreement was found for these three parameters and their previously measured values. The effective impedance of the backing material, however, was measured as $Z_B = 4.0 \times 10^6$ kg/m²sec, or 21% higher than its value before bonding the ceramic onto it. This effective backing impedance is used in deriving the theoretical curves to be shown later in this paper.

The specified matching layer was cast on the front of the PZT disk using a room temperature curing alumina/epoxy composite material developed for this purpose. The measured value for the matching layer material was 3.49×10^6 kg/m²sec. The desired value was 3.45×10^6 kg/m²sec. The actual thickness of the matching layer is hard to measure nondestructively and is assumed to be the desired value. The measured values of electrical impedance of the untuned transducer loaded by water is compared with theory in Fig. 3.

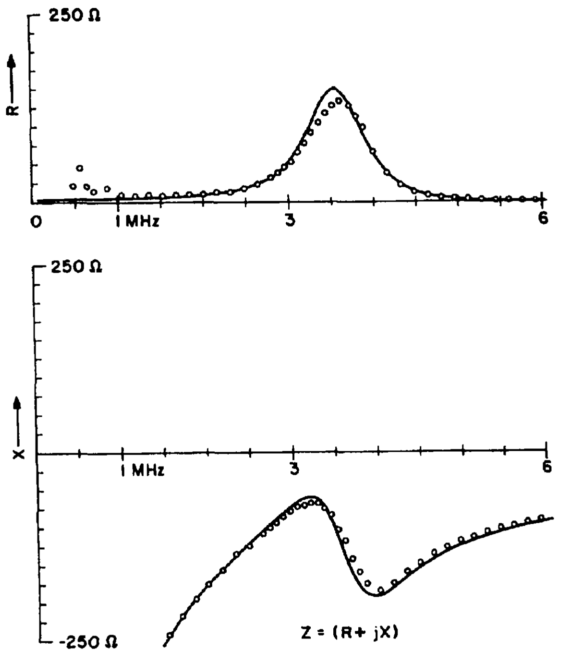

Fig. 3. Measured values of electrical impedance of untuned transducer compared with theory.

Next, the source and matching network was connected to the transducer, and all of the components were manually adjusted to obtain the best impulse response. This is shown in Fig. 4, together with the impulse response we were trying to obtain. The upper photograph shows very good agreement between the two. In Fig. 5, the same impulse response is shown, but with the vertical axis expanded by a factor of 10 . Here we can see the agreement is certainly less than perfect, though the 40 dB ringdown time is in fact about 1.5 μsec . Next, the insertion loss was measured at 21 frequencies around the center frequency (f_0 = 3.65 MHz). These values are plotted in Fig. 6 as open circles, and compared with theory (solid line). The typical 3 dB discrepancy between theory and experiment is evident.

The measured values of the adjusted matching parameters are

$$L_s = 4.1\ \mu H \qquad L_p = 5.7\ \mu H$$
$$C_p = 332\ pF \qquad R_s = 86\ \Omega \tag{11}$$

Using these adjusted values, the theoretical electrical impedance looking into the tuned transducer has been calculated and is plotted in Fig. 7 as solid lines. The measured electrical impedance is plotted as open circles. Again, we see good agreement between theory and experiment. We can also see that the tuning has reduced the reactive component of the transducer impedance as well as broadening the real part. It has also removed the effect of radial modes, seen as small, low-frequency peaks in Fig. 4.

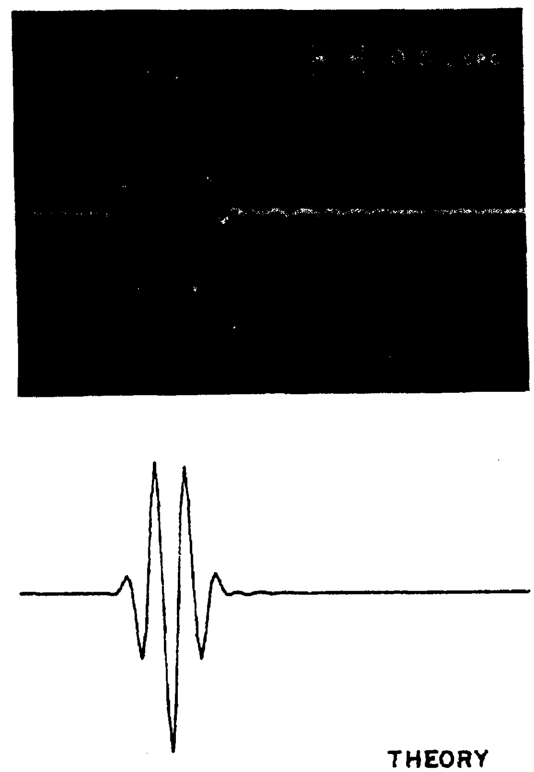

Fig. 4. Measured impulse response compared with theory.

Conclusion

We have shown that the computer optimized design techniques described in this paper can lead to considerably improved transient performance of bulk wave transducers. We have found that it is often necessary to make minor adjustments to the electrical components used in the design to obtain optimal performance. These adjustments, however, have been easy to make, and it has not been necessary to change the more fixed parameters such as matching layer thickness and impedance.

Another conclusion which can be drawn from this work is that it is appropriate to change our definition of optimum transducer response. In the past, a great deal of emphasis has been placed on the minimum insertion loss at the center frequency. What is of greater importance, in fact, is to reduce the overall insertion loss, or more precisely to increase the peak amplitude of the impulse response. This has been shown to be possible in work not reported here through the use of lighter backing impedances, and has been done with little to no degradation to the impulse response shape, while increasing the peak amplitude of the response by as much as 6 dB . Other work has shown that further improvements to both the shape and the amplitude of the impulse response can be made through the use of multiple

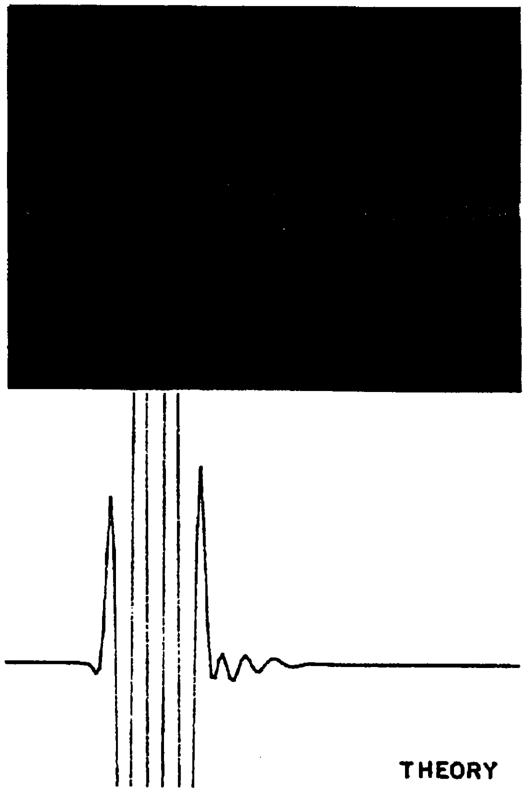

Fig. 5. Measured impulse response compared with theory. Vertical axis is expanded by 10.

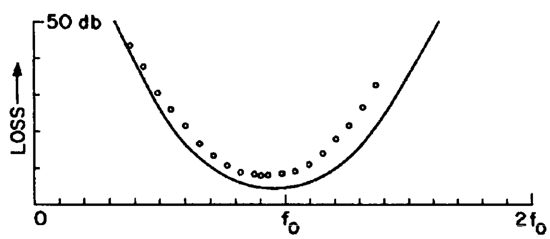

Fig. 6. Measured insertion loss compared with theory.

matching layer schemes. In these cases, the use of computer optimized design techniques have become even more important due to the increased number of design variables.

The true power of these techniques, however, can best be appreciated when lossy load media, complex load impedances, the effect of transmission lines, non-ideal transformers, etc. can be modeled, and successfully compensated for in the transducer design.

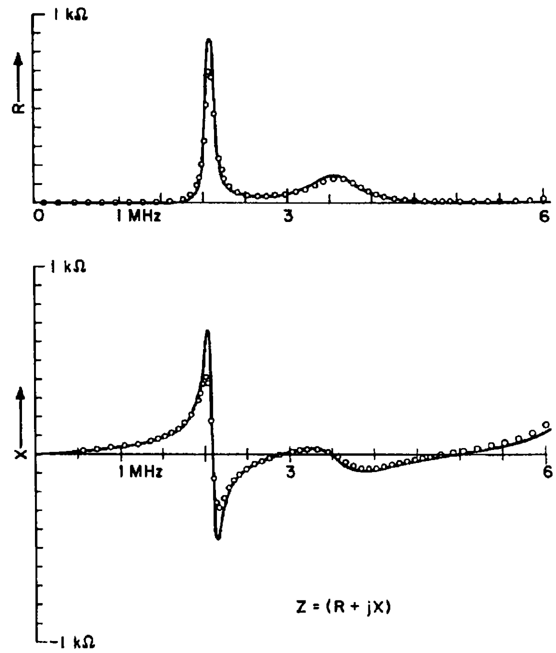

Fig. 7. Measured value of electrical impedance of tuned transducer.

References

1. D. C. Youla, "A New Theory of Broadband Matching," IEEE Trans. Cir. Theory, CT-11, 30, 1964.
2. R. M. Fano, "Theoretical Limitations on the Broadband Matching of Arbitrary Impedances," J. Franklin Institute, 244, 57, 139, 1950.
3. T. M. Reeder, W. R. Shreve, and P. L. Adams, "A New Broadband Coupling Network for Interdigital Surface Wave Transducers," IEEE Trans. Sonics and Ultrasonics, SU-19, 466, 1972.
4. J. Anderson and L. Wilkins, "The Design of Optimum Lumped Broadband Equalizers for Ultrasonic Transducers," J. Acous. Soc., 66, 629, 1979.
5. C. DeSilets, J. Fraser, and G. Kino, "The Design of Efficient Broadband Piezoelectric Transducers," IEEE Trans. Sonics and Ultrasonics, 25, 115, 1978.
6. D. Leedom, R. Krimholtz, and G. Matthaei, "Equivalent Circuits for Transducers Having Arbitrary Even or Odd Symmetry Piezoelectric Excitation," IEEE Trans. Sonics and Ultrasonics, SU-18, 128-141, July, 1971.

Acknowledgment

This work was supported by the National Science Foundation and the Department of Energy under Contract No. DE-AM03-76SF00326.